Functional MRI brain state occupancy in the presence of cerebral small vessel disease – pre-registration for a replication analysis of the Hamburg City Health Study

Eckhard Schlemm, MBBS PhD [1] ✉ **and Thies Ingwersen, MD** [1]

[1]Department of Neurology, University Medical Center Hamburg-Eppendorf

✉ **For correspondence:** e.schlemm@uke.de

Present address: Dr. Dr. Eckhard Schlemm, Klinik und Poliklinik für Neurologie, Universitätsklinikum Hamburg-Eppendorf, Martinistr. 52, D-20251 Hamburg

Data availability: Preprocessed data will be available e.g. on https://github.com/csi-hamburg/HCHS-brain-states-RR.

Funding: Deutsche Forschungsgemeinschaft (DFG) – 178316478 – C2

Competing interests: The author declares no competing interests.

Abstract

Objective: To replicate recent findings about the association between the extent of cerebral small vessel disease (cSVD), functional brain network dedifferentiation and cognitive impairment.

Methods: We will analyze demographic, imaging and behavioral data from the prospective population-based Hamburg City Health Study. Using a fully prespecified analysis pipeline, we will estimate discrete brain states from structural and resting-state functional magnetic resonance imaging (MRI). In a multiverse analysis we will vary brain parcellations and functional MRI confound regression strategies. Severity of cSVD will be operationalised as the volume of white matter hyperintensities of presumed vascular origin. Processing speed and executive dysfunction are quantified by the trail making test (TMT).

Hypotheses: We hypothesize a) that greater volume of supratentorial white matter

hyperintensities is associated with less time spent in functional MRI-derived brain states of high fractional occupancy; and b) that less time spent in these high-occupancy brain states is associated with longer time to completion in part B of the TMT.

Introduction

Cerebral small vessel disease (cSVD) is an arteriolopathy of the brain, associated with age and common cardiovascular risk factors (Wardlaw, C. Smith, and Dichgans, 2013). cSVD predisposes to ischemic, in particular lacunar, stroke and may lead to cognitive impairment and dementia (Cannistraro et al., 2019). Neuroimaging findings in cSVD reflect its underlying pathology (Wardlaw, Valdés Hernández, and Muñoz-Maniega, 2015) and include white matter hyperintensities (WMH) and lacunes of presumed vascular origin, small subcortical infarcts and microbleeds, enlarged perivascular spaces as well as brain atrophy (Wardlaw, E. E. Smith, et al., 2013). However, the extent of visible cSVD features on magnetic resonance imaging (MRI) is an imperfect predictor of the severity of clinical sequelae (Das et al., 2019), and our understanding of the causal mechanisms linking cSVD-associated brain damage to clinical deficits remains limited (Bos et al., 2018).

Recent efforts have concentrated on exploiting network aspects of the structural (Tuladhar, Dijk, et al., 2016; Tuladhar, Tay, et al., 2020; Lawrence, Zeestraten, et al., 2018) and functional (Dey et al., 2016; Schulz et al., 2021) organization of the brain to understand the relation between cSVD and clinical deficits in cognition and other domains reliant on distributed processing. Reduced structural network efficiency has repeatedly been described as a causal factor in the development of cognitive impairment, in particular executive dysfunction and reduced processing speed, in cSVD (Lawrence, Chung, et al., 2014; Shen et al., 2020; Reijmer et al., 2016; Prins et al., 2005). Findings with respect to functional connectivity ~~results~~(FC), on the other hand, are more heterogeneous ~~, perhaps due to its limited reproducibility in~~ than their SC counterparts, perhaps because FC measurements are prone to be affected by hemodynamic factors and noise, resulting in relatively low reliability, especially with resting-state scans of short duration (Laumann, Gordon, et al., 2015). This problem is exacerbated in the presence of cSVD and ~~dependence on~~ made worse by the arbitrary processing choices (Lawrence, Tozer, et al., 2018; Gesierich et al., 2020).

As a promising new avenue, time-varying, or dynamic, functional connectivity approaches

have more recently been explored in patients with subcortical ischemic vascular disease (Yin et al., 2022; Xu et al., 2021). While the study of dynamic FC measures may not solve the problem of limited reliability, especially in small populations or subjects with extensive structural brain changes, it adds another – temporal – dimension to the study of functional brain organisation, which is otherwise overlooked. Importantly, FC dynamics do not only reflect moment-to-moment fluctuations in cognitive processes but are also related to brain plasticity and homeostasis (Laumann and Snyder, 2021; Laumann, Snyder, et al., 2017), which may be impaired in cSVD.

In the present paper, we aim to replicate and extend the main results of (Schlemm et al., 2022); in this recent study, the authors analyzed MR imaging and clinical data from the prospective Hamburg City Health Study (HCHS, (Jagodzinski et al., 2020)) using a coactivation pattern approach to define discrete brain states and found associations between the WMH load, time spent in high-occupancy brain states characterized by activation or suppression of the default mode network (DMN) and ~~executive dysfunction~~cognitive impairment.

The fractional occupancy of a functional MRI-derived discrete brain state is a subject-specific measure of brain dynamics defined as the proportion of BOLD volumes assigned to that state relative to all BOLD volumes acquired during a resting-state scan.

Our primary hypothesis is that the volume of supratentorial white matter hyperintensities is associated with the fractional occupancy ~~(defined below)~~ of DMN-related brain states in a middle-aged to elderly population mildly affected by cSVD. Our second hypothesis is that this fractional occupancy is associated with executive dysfunction and reduced processing speed, measured as the time to complete part B of the trail making test (TMT).

Both hypotheses will be tested in an independent subsample of the HCHS study population using the same imaging protocols, examination procedures and analysis pipelines as in (Schlemm et al., 2022). The robustness of associations will be explored in a multiverse approach by varying key steps in the analysis pipeline.

Methods

Study population

The paper will analyze data from the Hamburg City Health Study (HCHS), which is an ongoing prospective, population-based cohort study aiming to recruit a cross-sectional

Question	Hypothesis	Sampling plan	Analysis plan	Rationale for deciding the sensitivity of the test	Interpretation given different outcomes	Theory that could be shown wrong by the outcome
Is severity of cerebral small disease, quantified by the volume of supratentorial white matter hyperintensities of presumed vascular origin (WMH), associated with time spent in high-occupancy brain states, defined by resting-state functional MRI	Higher WMH volume is associated with lower average occupancy of the two highest-occupancy brain states.	Available subjects with clinical and imaging data from the the HCHS (Jagodzinski et al., 2020)	Standardized preprocessing of structural and functional MRI data • automatic quantification of WMH • co-activation pattern analysis • multivariable generalised regression analyses	Tradition	$P < 0.05$ –> rejection of the null hypothesis of no association between cSVD and fractional occupancy; $P > 0.05$ –> insufficient evidence to reject the null hypothesis	Functional brain dynamics are not related to subcortical ischemic vascular disease.

Table 1. Study Design Template

sample of $45\,000$ adult participants from the city of Hamburg, Germany (Jagodzinski et al., 2020). From the first $10\,000$ participants of the HCHS we will aim to include those who were documented to have received brain imaging (n=2652) and exclude those who were analyzed in our previous report (Schlemm et al., 2022) (n=988), for an expected sample size of approximately 1500 participants. The ethical review board of the Landesärztekammer Hamburg (State of Hamburg Chamber of Medical Practitioners) approved the HCHS (PV5131), all participants provided written informed consent.

Demographic and clinical characterization

From the study database we will extract participants' age at the time of inclusion in years, their ~~self-reported gender~~ sex and the number of years spent in education. During the visit at the study center, participants undergo cognitive assessment using standardized tests. We will extract from the database their performance scores in the Trail Making Test part B, measured in seconds, as an operationalization of executive function and psychomotor processing speed (Tombaugh, 2004; Arbuthnott and Frank, 2000).

MRI acquisition and preprocessing

The magnetic resonance imaging protocol for the HCHS includes structural and resting-state functional sequences. The acquisition parameters on a $3\,\mathrm{T}$ Siemens Skyra MRI scanner (Siemens, Erlangen, Germany) have been reported before (Petersen et al., 2020; Frey et al., 2021) and are given as follows:

For T_1-weighted anatomical images, a 3D rapid acquisition gradient-echo sequence (MPRAGE) was used with the following sequence parameters: ~~repettion~~ repetition time TR $= 2500\,\mathrm{ms}$, echo time TE $= 2.12\,\mathrm{ms}$, 256 axial slices, slice thickness ST $= 0.94\,\mathrm{mm}$, and in-plane resolution IPR $= (0.83 \times 0.83)\,\mathrm{mm}^2$.

T_2-weighted fluid attenuated inversion recovery (FLAIR) images were acquired with the following sequence parameters: TR = 4700 ms, TE = 392 ms, 192 axial slices, ST = 0.9 mm, IPR = $(0.75 \times 0.75)\,\mathrm{mm}^2$.

125 resting state functional MRI volumes were acquired (TR = 2500 ms; TE = 25 ms; flip angle = 90°; slices = 49; ST = 3 mm; slice gap = 0 mm; IPR = $(2.66 \times 2.66)\,\mathrm{mm}^2$). Subjects were asked to keep their eyes open and to think of nothing.

We will verify the presence and voxel-dimensions of expected MRI data for each participant and exclude those for whom at least one of T_1-weighted, FLAIR and resting-state MRI is missing. We will also exclude participants with a neuroradiologically confirmed space-occupying intra-axial lesion. To ensure reproducibility, no visual quality assessment on raw images will be performed.

For the remaining participants, structural and resting-state functional MRI data will be preprocessed using FreeSurfer v6.0 (https://surfer.nmr.mgh.harvard.edu/), and fmriPrep v20.2.6 (Esteban et al., 2019), using default parameters. Participants will be excluded if automated processing using at least one of these packages fails.

Quantification of WMH load

For our primary analysis, the extent of ischemic white matter disease will be operationalized as the total volume of supratentorial WMHs obtained from automated segmentation using a combination of anatomical priors, BIANCA (Griffanti, Zamboni, et al., 2016) and LOCATE (Sundaresan et al., 2019), post-processed with a minimum cluster size of 30 voxels, as described in (Schlemm et al., 2022). In an exploratory analysis, we partition voxels identified as WMH into deep and periventricular components according to their distance to the ventricular system (cut-off 10 mm, (Griffanti, Jenkinson, et al., 2018))

Brain state estimation

Output from fMRIprep will be post-processed using xcpEngine v1.2.1 to obtain de-confounded spatially averaged BOLD time series (Ciric, Wolf, et al., 2017). For the primary analysis we will use the *36p* regression strategy and the Schaefer-400 parcellation (Schaefer et al., 2018), as in (Schlemm et al., 2022).

Different atlases and confound regression strategies, as implemented in xcpEngine, will be included in the exploratory multiverse analysis.

Co-activation pattern (CAP) analysis will be performed by first aggregating parcellated, de-confounded BOLD signals into a $\left(n_{\text{parcels}} \times \sum_i n_{\text{time points},i}\right)$ feature matrix, where $n_{\text{time points},i}$

denotes the number of retained volumes for subject i after confound regression. Clustering will be performed using the k-means algorithm ($k = 5$) with distance measure given by 1 minus the sample Pearson correlation between points, as implemented in Matlab R2021a. We will estimate subject- and state-specific fractional occupancies, which are defined as the proportion of BOLD volumes assigned to each brain state (Vidaurre et al., 2018). The two states with the highest average occupancy will be identified as the basis for further analysis.

Statistical analysis

For demographic (age, ~~gender~~sex, years of education) and clinical (TMT-B) variables the number of missing records will be reported. For non-missing values, we will provide descriptive summary statistics using median and interquartile range. The proportion of men and women in the sample will be reported. Regression modelling will be carried out as a complete-case analysis.

As a first outcome-neutral quality check of the implementation of the MRI processing pipeline, brain state estimation and co-activation pattern analysis, we will compare fractional occupancies between brain states. We expect that the average fractional occupancy in two high-occupancy states is higher than the average fractional occupancy in the other three states. Point estimates and 95% confidence intervals will be presented for the difference in average fractional occupancy to check this assertion.

For further analyses, non-zero WMH volumes will be subjected to a logarithmic transformation. Zero values will retain their value zero; to compensate, all models will include a binary indicator for zero WMH volume if at least one non-zero value is present.

To assess the primary hypothesis of a negative association between the extent of ischemic white matter disease and time spent in high-occupancy brain states, we will perform a fixed-dispersion beta-regression to model the logit of the conditional expectation of the average fractional occupancy of two high-occupancy states as an affine function of the logarithmized WMH load. Age and ~~gender~~ sex will be included as covariates. The strength of the association will be quantified as an odds ratio per interquartile ratio of the WMH burden distribution and accompanied by a 95% confidence interval. Significance testing of the null hypothesis of no association will be conducted at the conventional significance level of 0.05. Estimation and testing will be carried out using the 'betareg' package v3.1.4 in R v4.2.1.

To assess the secondary hypothesis of an association between time spent in high-

occupancy brain states and executive dysfunction, we will perform a generalized linear regression with a Gamma response distribution to model the logarithm of the conditional expected completion time in part B of the TMT as an affine function of the average fractional occupancy of two high-occupancy states. Age, ~~gender~~sex, years of education and logarithmized WMH load will be included as covariates. The strength of the association will be quantified as a multiplicative factor per percentage point and accompanied by a 95% confidence interval. Significance testing of the null hypothesis of no association will be conducted at the conventional significance level of 0.05. Estimation and testing will be carried out using the glm function included in the 'stats' package from R v4.2.1.

Sample size calculation is based on ~~the data presented in , where an odds ratio of was reported as the primary~~ an effect size on the odds ratio scale of 0.95, corresponding to an absolute difference in the probability of occupying a DMN-related brain state between the first and third WMH-load quartile of 1.3 percentage points, and between the 5% and 95% percentile of 3.1 percentage points. Approximating half the difference in fractional occupancy of DMN-related states between different task demands (rest vs n-back) in healthy subjects, which was estimated to lie between 6 and 7 percentage points (Cornblath et al., 2020), this value represent a plausible choice for the smallest effect size of ~~interest~~theoretical and practical interest. It also equals the effect size estimated based on the data presented in (Schlemm et al., 2022).

We used simple bootstrapping to create $10\,000$ hypothetical datasets of size 200, 400, 600, 800, 900, 910, …, 1100, 1200, 1400, 1500, 1600. Each dataset was subjected to the estimation procedure described above. For each sample size, the proportion of datasets in which the primary null hypothesis of no association between fractional occupancy and WMH load could be rejected at $\alpha = 0.05$ was computed and is recorded as a power curve in Figure 1.

It is seen that a sample size of 960 would allow replication of the reported effect with a power of $80.2\,\%$. We anticipate a sample size of 1500, which yields a power of $93.9\,\%$.

Multiverse analysis

Both in (Schlemm et al., 2022) and for our primary replication analysis we made certain analytical choices in the ~~operationalisation~~ operationalization of brain states and ischemic white matter disease, namely the use of the *36p* confound regression strategy, the Schaefer-400 parcellation and a BIANCA/LOCATE-based WMH segmentation algorithm. ~~If the hypothesized~~ The robustness of the association between WMH burden

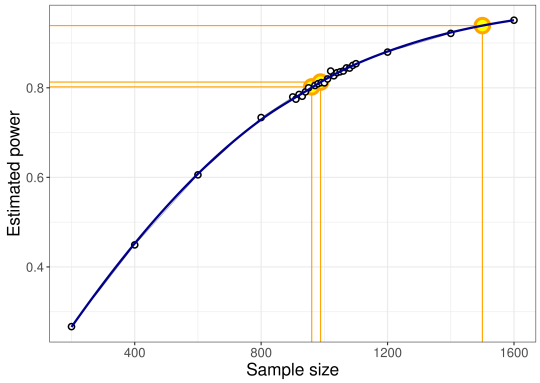

Figure 1. Estimated power for different sample sizes is obtained as the proportion of synthetic data sets in which the null hypothesis of no association between WMH volume and time spent in high-occupancy brain states an be rejected at the $\alpha = 0.05$ significance level. Proportions are based on a total of 10 000 synthetic data sets obtained by bootstrapping the data presented in (Schlemm et al., 2022). Highlighted in orange are the smallest sample size ensuring a power of at least 80 % ($n = 960$), the sample size of the pilot data ($n = 988$, post-hoc power 81.3 %), and the expected sample sample size for this replication study ($n = 1500$, a-priori power 93.9 %).

Name of the atlas	#parcels	Reference
Desikan–Killiany	86	Desikan et al., 2006
AAL	116	Tzourio-Mazoyer et al., 2002
Harvard–Oxford	112	Makris et al., 2006
glasser360	360	Glasser et al., 2016
gordon333	333	Gordon et al., 2016
power264	264	Power, Cohen, et al., 2011
schaefer{N}	100 200 400	Schaefer et al., 2018

AAL: Automatic Anatomical Labelling

(a) Parcellations

Design	Reference
24p	Friston et al., 1996
24p + GSR	Macey et al., 2004
36p	Satterthwaite et al., 2013
~~26p~~ 36p + spike regression	Cox, 1996
36p + despiking	Satterthwaite et al., 2013
36p + scrubbing	Power, Mitra, et al., 2014
aCompCor	Muschelli et al., 2014
tCompCor	Behzadi et al., 2007
AROMA	Pruim et al., 2015

GSR: Global signal regression, AROMA: ~~bla~~ Automatic Removal of Motion Artifacts

(b) Confound regression strategies, adapted from (Ciric, Wolf, et al., 2017)

Table 2. Multiverse analysis, implemented using xcpEngine (Ciric, Rosen, et al., 2018)

and time spent in high-occupancy states ~~can be replicated using these primary analytical choices, its robustness~~ with regard to other choices will be explored in a multiverse analysis (Steegen et al., 2016). Specifically, in an exploratory analysis, we will estimate brain states from BOLD time series processed according to a variety of established confound regression strategies and aggregated over different cortical brain parcellations (Table 2, Ciric, Rosen, et al., 2018; Ciric, Wolf, et al., 2017). Extent of cSVD will additionally be quantified by the volume of deep and periventricular white matter hyperintensities.

For each combination of analytical choice of confound regression strategy, parcellation and subdivision of white matter lesion load ($9 \times 9 \times 3 = 243$ scenarios in total) we will quantify the association between WMH load and average time spent in high-occupancy brain states using odds ratio and 95 % confidence intervals as described above.

No hypothesis testing and ~~, therefore, no adjustment for multiple testing,~~ will be

carried out in these ~~non-primary analyses.~~ multiverse analyses. They rather serve to inform about the robustness of the outcome of the test of the primary hypothesis. Any substantial conclusions about the association between severity of cerebral small pathology and time spent in high-occupancy brain states, as stated in the Scientific Question in Table 1, will be drawn from the primary analysis using pre-specified methodological choices.

~~Exploratory~~ Further exploratory analysis

In previous work, two high-occupancy brain states were related to the default-mode network (Cornblath et al., 2020). We will further explore this relation by computing, for each individual brain state, the cosine similarity of the positive and negative activations of the cluster's centroid with a set of a-priori defined functional 'communities' or networks (Schaefer et al., 2018; Yeo et al., 2011). Results will be thus visualized as spider plots for the Schaefer, Gordon and Power ~~atlasses~~atlases.

In further exploratory analyses we plan to describe the associations between brain state dynamics and other measures of cognitive ability, such as memory and language.

Code and pilot data

Summary data from the first 1000 imaging data points of the HCHS have been published with (Schlemm et al., 2022) and form the basis for the hypotheses tested in this replication study. We have implemented our prespecified analysis pipeline described above in R and Matlab, and applied it to this previous sample. Data, code and results have been stored on GitHub (https://github.com/csi-hamburg/HCHS_brain_states_RR) und preserved on Zenodo.

Thus re-analysing data from 988 subjects, the separation between two high-occupancy and three low-occupancy brain states could be reproduced for all combinations of brain parcellation and confound regression strategies (Figure 2).

In a multiverse analysis, the main finding was somewhat robust with respect to these choices: a statistically significant negative association between WMH load and time spent in high-occupancy states was observed in 18/81 scenarios, with 5/81 statistically significant positive associations occurring with the Desikan–Killiany parcellation only (Figure 3).

The secondary finding of an association between greater TMT-B times and lower fractional occupancy was similarly robust with 12/81 statistically significant negative and no

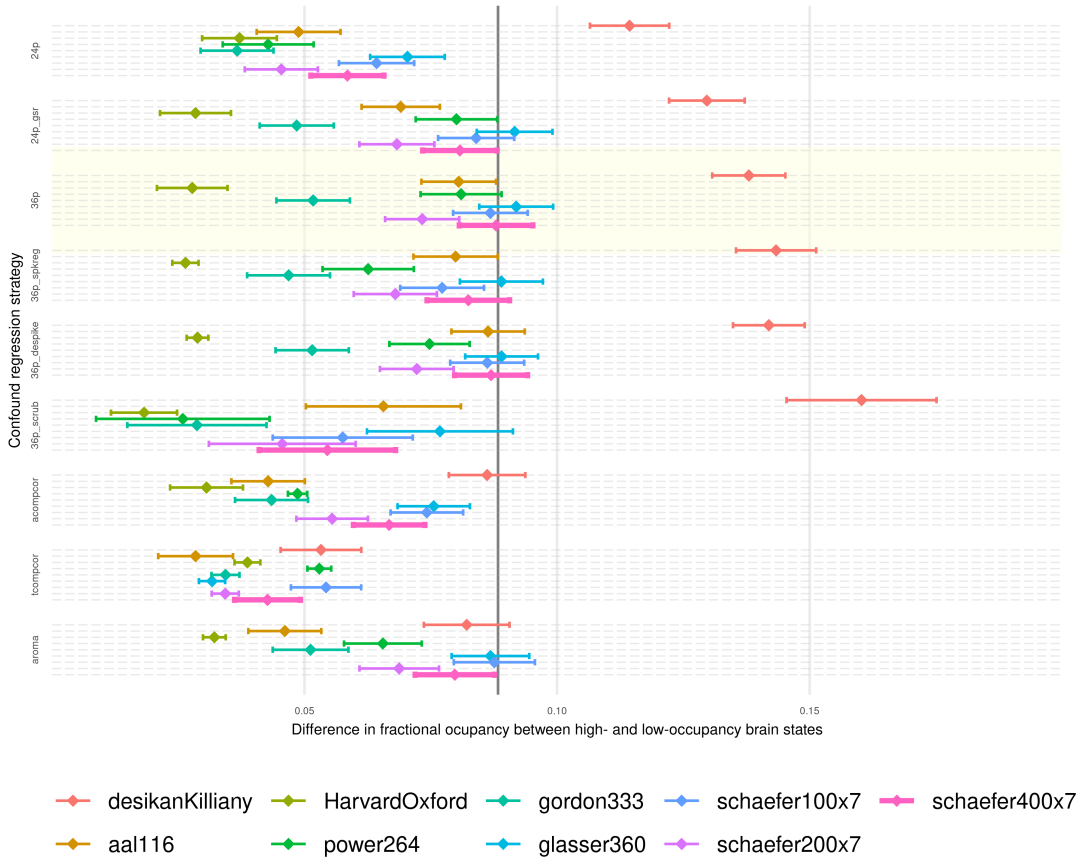

Figure 2. Point estimates (dots) and 95 % confidence intervals (line segments) for the mean difference in fractional occupancy between high- and low occupancy states are shown for different confound regression strategies (groups along the vertical axis) and brain parcellations (color). The difference in FO for a particular choice of regression strategy and brain parcellation is nominally statistically significantly different from zero at a significance level of 5% if the corresponding interval does not contain zero. Hence, the FO difference is significant for *all* processing choices, reflecting the separation between high- und low-occupancy states. The primary choices (*36p* and *schaefer400*) are highlighted by a yellow box and thick pink line, respectively. The effect size reported in (Schlemm et al., 2022) is indicated by a vertical line at 0.08830623.

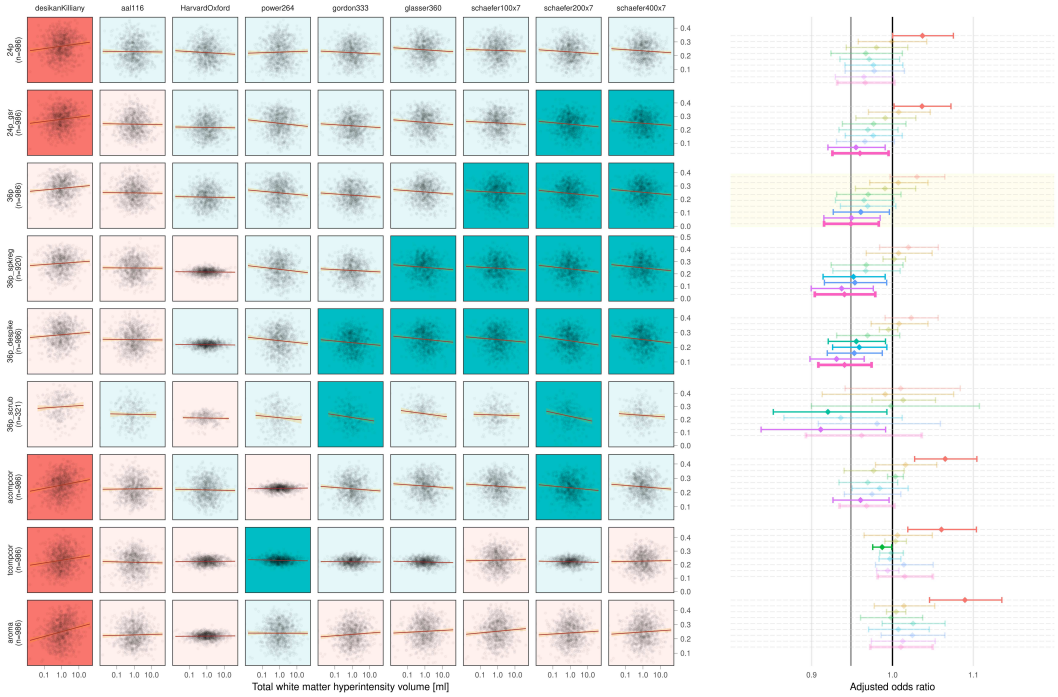

Figure 3. On the left, scatter plots of average fractional occupancies in high-occupancy states against WMH volume on a logarithmic scale (base 10 for easier visualization) for different combinations of confound regression strategies and brain parcellations. Linear regression lines indicate the direction of the unadjusted association between log(WMH) and occupancy. Background color of individual panels indicates the direction of the association after adjustment for age, sex and zero WMH volume (green, negative; red, positive). A pale background indicates that the association between log(WMH) and average occupancy is not statistically different from zero. On the right, the same information is shown using point estimates and 95 % confidence intervals for the adjusted odds ratio of the association.

statistically significant positive associations.

Timeline and access to data

At the time of planning of this study, all demographic, clinical and imaging data used in this analysis have been collected by the HCHS and are held in the central trial database. Quality checks for non-imaging variables have been performed centrally. WMH segmentation based on structural MRI data of the first 10 000 participants of the HCHS has been performed previously using the BIANCA/LOCATE approach (Rimmele et al., 2022) and results are included in this preregistration (~~./derivaties/WMH/cSVD_all.csv~~./derivatives/WMH/cS
Functional MRI data and clinical measures of executive dysfunction (TMT-B scores) have not been analyzed by the author. Analysis of the data will begin immediately after acceptance-in-principle of the stage 1 submission of the registered report is obtained. Submission of the full manuscript (stage 2) is planned two months later.

Acknowledgment

This preprint was created using the LaPreprint template (https://github.com/roaldarbol/lapreprint) by Mikkel Roald-Arbøl .

References

Arbuthnott, Katherine and Janis Frank (2000). "Trail making test, part B as a measure of executive control: validation using a set-switching paradigm". In: *Journal of clinical and experimental neuropsychology* 22.4, pp. 518–528.

Behzadi, Yashar et al. (2007). "A component based noise correction method (CompCor) for BOLD and perfusion based fMRI". In: *Neuroimage* 37.1, pp. 90–101.

Bos, Daniel et al. (2018). "Cerebral small vessel disease and the risk of dementia: A systematic review and meta-analysis of population-based evidence". en. In: *Alzheimers. Dement.* 14.11, pp. 1482–1492.

Cannistraro, Rocco J et al. (2019). "CNS small vessel disease: A clinical review". en. In: *Neurology* 92.24, pp. 1146–1156.

Ciric, Rastko, Adon FG Rosen, et al. (2018). "Mitigating head motion artifact in functional connectivity MRI". In: *Nature protocols* 13.12, pp. 2801–2826.

Ciric, Rastko, Daniel H Wolf, et al. (2017). "Benchmarking of participant-level confound regression strategies for the control of motion artifact in studies of functional connectivity". en. In: *Neuroimage* 154, pp. 174–187.

283 Cornblath, Eli J et al. (2020). "Temporal sequences of brain activity at rest are constrained
284 by white matter structure and modulated by cognitive demands". en. In: *Commun Biol*
285 3.1, p. 261.
286 Cox, Robert W (1996). "AFNI: software for analysis and visualization of functional mag-
287 netic resonance neuroimages". In: *Computers and Biomedical research* 29.3, pp. 162–
288 173.
289 Das, Alvin S et al. (2019). "Asymptomatic Cerebral Small Vessel Disease: Insights from
290 Population-Based Studies". en. In: *J. Stroke Cerebrovasc. Dis.* 21.2, pp. 121–138.
291 Desikan, Rahul S et al. (2006). "An automated labeling system for subdividing the human
292 cerebral cortex on MRI scans into gyral based regions of interest". In: *Neuroimage* 31.3,
293 pp. 968–980.
294 Dey, Ayan K et al. (2016). "Pathoconnectomics of cognitive impairment in small vessel
295 disease: A systematic review". en. In: *Alzheimers. Dement.* 12.7, pp. 831–845.
296 Esteban, Oscar et al. (2019). "fMRIPrep: a robust preprocessing pipeline for functional
297 MRI". en. In: *Nat. Methods* 16.1, pp. 111–116.
298 Frey, Benedikt M et al. (2021). "White matter integrity and structural brain network topol-
299 ogy in cerebral small vessel disease: The Hamburg city health study". en. In: *Hum. Brain*
300 *Mapp.* 42.5, pp. 1406–1415.
301 Friston, Karl J et al. (1996). "Movement-related effects in fMRI time-series". In: *Magnetic*
302 *resonance in medicine* 35.3, pp. 346–355.
303 Gesierich, Benno et al. (2020). "Alterations and test-retest reliability of functional connec-
304 tivity network measures in cerebral small vessel disease". en. In: *Hum. Brain Mapp.*
305 41.10, pp. 2629–2641.
306 Glasser, Matthew F et al. (2016). "A multi-modal parcellation of human cerebral cortex".
307 en. In: *Nature* 536.7615, pp. 171–178.
308 Gordon, Evan M et al. (2016). "Generation and Evaluation of a Cortical Area Parcellation
309 from Resting-State Correlations". en. In: *Cereb. Cortex* 26.1, pp. 288–303.
310 Griffanti, Ludovica, Mark Jenkinson, et al. (2018). "Classification and characterization of
311 periventricular and deep white matter hyperintensities on MRI: A study in older adults".
312 en. In: *Neuroimage* 170, pp. 174–181.
313 Griffanti, Ludovica, Giovanna Zamboni, et al. (2016). "BIANCA (Brain Intensity AbNormal-
314 ity Classification Algorithm): A new tool for automated segmentation of white matter
315 hyperintensities". en. In: *Neuroimage* 141, pp. 191–205.

316 Jagodzinski, Annika et al. (2020). “Rationale and Design of the Hamburg City Health Study”.
317 en. In: *Eur. J. Epidemiol.* 35.2, pp. 169–181.
318 Laumann, Timothy O, Evan M Gordon, et al. (2015). “Functional system and areal organi-
319 zation of a highly sampled individual human brain”. In: *Neuron* 87.3, pp. 657–670.
320 Laumann, Timothy O and Abraham Z Snyder (2021). “Brain activity is not only for thinking”.
321 In: *Current Opinion in Behavioral Sciences* 40, pp. 130–136.
322 Laumann, Timothy O, Abraham Z Snyder, et al. (2017). “On the stability of BOLD fMRI
323 correlations”. In: *Cerebral cortex* 27.10, pp. 4719–4732.
324 Lawrence, Andrew J, Ai Wern Chung, et al. (2014). “Structural network efficiency is as-
325 sociated with cognitive impairment in small-vessel disease”. en. In: *Neurology* 83.4,
326 pp. 304–311.
327 Lawrence, Andrew J, Daniel J Tozer, et al. (2018). “A comparison of functional and trac-
328 tography based networks in cerebral small vessel disease”. en. In: *Neuroimage Clin* 18,
329 pp. 425–432.
330 Lawrence, Andrew J, Eva A Zeestraten, et al. (2018). “Longitudinal decline in structural
331 networks predicts dementia in cerebral small vessel disease”. en. In: *Neurology* 90.21,
332 e1898–e1910.
333 Macey, Paul M et al. (2004). “A method for removal of global effects from fMRI time series”.
334 In: *Neuroimage* 22.1, pp. 360–366.
335 Makris, Nikos et al. (2006). “Decreased volume of left and total anterior insular lobule in
336 schizophrenia”. In: *Schizophrenia research* 83.2-3, pp. 155–171.
337 Muschelli, John et al. (2014). “Reduction of motion-related artifacts in resting state fMRI
338 using aCompCor”. In: *Neuroimage* 96, pp. 22–35.
339 Petersen, Marvin et al. (2020). “Network Localisation of White Matter Damage in Cerebral
340 Small Vessel Disease”. en. In: *Sci. Rep.* 10.1, p. 9210.
341 Power, Jonathan D, Alexander L Cohen, et al. (2011). “Functional network organization of
342 the human brain”. en. In: *Neuron* 72.4, pp. 665–678.
343 Power, Jonathan D, Anish Mitra, et al. (2014). “Methods to detect, characterize, and re-
344 move motion artifact in resting state fMRI”. In: *Neuroimage* 84, pp. 320–341.
345 Prins, Niels D et al. (2005). “Cerebral small-vessel disease and decline in information pro-
346 cessing speed, executive function and memory”. en. In: *Brain* 128.Pt 9, pp. 2034–2041.
347 Pruim, Raimon HR et al. (2015). “ICA-AROMA: A robust ICA-based strategy for removing
348 motion artifacts from fMRI data”. In: *Neuroimage* 112, pp. 267–277.

Reijmer, Yael D et al. (2016). “Small vessel disease and cognitive impairment: The relevance of central network connections”. en. In: *Hum. Brain Mapp.* 37.7, pp. 2446–2454.

Rimmele, David Leander et al. (2022). “Association of Carotid Plaque and Flow Velocity With White Matter Integrity in a Middle-aged to Elderly Population”. en. In: *Neurology*.

Satterthwaite, Theodore D et al. (2013). “An improved framework for confound regression and filtering for control of motion artifact in the preprocessing of resting-state functional connectivity data”. In: *Neuroimage* 64, pp. 240–256.

Schaefer, Alexander et al. (2018). “Local-Global Parcellation of the Human Cerebral Cortex from Intrinsic Functional Connectivity MRI”. en. In: *Cereb. Cortex* 28.9, pp. 3095–3114.

Schlemm, Eckhard et al. (2022). “Equalization of Brain State Occupancy Accompanies Cognitive Impairment in Cerebral Small Vessel Disease”. en. In: *Biol. Psychiatry* 92.7, pp. 592–602.

Schulz, Maximilian et al. (2021). “Functional connectivity changes in cerebral small vessel disease - a systematic review of the resting-state MRI literature”. en. In: *BMC Med.* 19.1, p. 103.

Shen, Jun et al. (2020). “Network Efficiency Mediates the Relationship Between Vascular Burden and Cognitive Impairment: A Diffusion Tensor Imaging Study in UK Biobank”. en. In: *Stroke* 51.6, pp. 1682–1689.

Steegen, Sara et al. (2016). “Increasing Transparency Through a Multiverse Analysis”. en. In: *Perspect. Psychol. Sci.* 11.5, pp. 702–712.

Sundaresan, Vaanathi et al. (2019). “Automated lesion segmentation with BIANCA: Impact of population-level features, classification algorithm and locally adaptive thresholding”. en. In: *Neuroimage* 202, p. 116056.

Tombaugh, Tom N (2004). “Trail Making Test A and B: normative data stratified by age and education”. en. In: *Arch. Clin. Neuropsychol.* 19.2, pp. 203–214.

Tuladhar, Anil M, Ewoud van Dijk, et al. (2016). “Structural network connectivity and cognition in cerebral small vessel disease”. en. In: *Hum. Brain Mapp.* 37.1, pp. 300–310.

Tuladhar, Anil M, Jonathan Tay, et al. (2020). “Structural network changes in cerebral small vessel disease”. en. In: *J. Neurol. Neurosurg. Psychiatry* 91.2, pp. 196–203.

Tzourio-Mazoyer, Nathalie et al. (2002). “Automated anatomical labeling of activations in SPM using a macroscopic anatomical parcellation of the MNI MRI single-subject brain”. In: *Neuroimage* 15.1, pp. 273–289.

Vidaurre, Diego et al. (2018). “Discovering dynamic brain networks from big data in rest and task”. en. In: *Neuroimage* 180.Pt B, pp. 646–656.

Wardlaw, Joanna M, Colin Smith, and Martin Dichgans (2013). “Mechanisms of sporadic cerebral small vessel disease: insights from neuroimaging”. en. In: *Lancet Neurol.* 12.5, pp. 483–497.

Wardlaw, Joanna M, Eric E Smith, et al. (2013). “Neuroimaging standards for research into small vessel disease and its contribution to ageing and neurodegeneration”. en. In: *Lancet Neurol.* 12.8, pp. 822–838.

Wardlaw, Joanna M, Maria C Valdés Hernández, and Susana Muñoz-Maniega (2015). “What are white matter hyperintensities made of? Relevance to vascular cognitive impairment”. en. In: *J. Am. Heart Assoc.* 4.6, p. 001140.

Xu, Yuanhang et al. (2021). “Altered Dynamic Functional Connectivity in Subcortical Ischemic Vascular Disease With Cognitive Impairment”. en. In: *Front. Aging Neurosci.* 13, p. 758137.

Yeo, B T Thomas et al. (2011). “The organization of the human cerebral cortex estimated by intrinsic functional connectivity”. en. In: *J. Neurophysiol.* 106.3, pp. 1125–1165.

Yin, Wenwen et al. (2022). “The Clustering Analysis of Time Properties in Patients With Cerebral Small Vessel Disease: A Dynamic Connectivity Study”. en. In: *Front. Neurol.* 13, p. 913241.